Bipolaron Hopping Conduction in Vacancy-Ordered Cs_2PtI_6 Perovskites

Vidya Raj,[ab] Abhishek Anand,[ab] Manasa Manoj,[ab] and Aravind Kumar Chandiran[ab*]

[a]Department of Chemical Engineering, Indian Institute of Technology Madras, Adyar, Chennai, Tamil Nadu, India 600036.

[b]Hyundai HTWO Innovation Centre, Indian Institute of Technology Madras, Adyar, Chennai, Tamil Nadu, India 600036.

* aravindkumar@iitm.ac.in

Electronic Supplementary Information

Experimental Section

Material Synthesis:

Cesium iodide (CsI, Spectrochem, 99.5%) and chloroplatinic acid hexahydrate ($H_2PtCl_6.6H_2O$, Sigma Aldrich, >37% Pt basis) were mixed in a 2:1 molar ratio and added to a Teflon reactor. Hydroiodic acid (HI, Qualigens) was then added to the mixture. The reactor was sealed and subjected to hydrothermal treatment at 170 °C for 6 hours. The resulting Cs_2PtI_6 powder was washed with ethanol three times and dried in a hot air oven at 70 °C for 12 hours.

Pellet Formation:

200 mg of Cs_2PtI_6 powder was pressed into a pellet using a die set and a hydraulic press (PCI Analytics) at a pressure of 2 tons.

Characterization:

The powder X-ray diffraction pattern was recorded using a Thermo Scientific Equinox 3000 with a Cu Kα radiation source. High-resolution micrographs were obtained using a Hitachi S-4800 scanning electron microscope. Fourier Transform Infrared Spectroscopy (FTIR) measurements were taken in the range of 4000-50 cm^{-1} using a JASCO 6600FV spectrometer with an ATR attachment. The spectrometer was operated under a complete vacuum for far-infrared measurements. The absorption onset of the sample was measured using a Shimadzu UV-2600 UV−Vis−NIR spectrophotometer equipped with a barium sulfate coated integrating sphere. Thermal decomposition of the samples was studied using a SDT Q600 (T.A. Instruments) with a temperature range from 25 °C to 900 °C at a rate of 10 °C/min under nitrogen. Phase transitions were analyzed using a NETZSCH DSC 204 F1 Phoenix differential scanning calorimeter. X-ray Photoelectron Spectroscopy (XPS) measurements were performed using an AXIS SUPRA instrument equipped with an Al Kα source at 1486.69 eV photon energy. The XPS data were analyzed using CASA XPS software, and all spectra were calibrated to the C *1s* peak at 284.6 eV. Temperature dependent Raman spectra were acquired using a Horiba-Yvon (HR-800UV) Raman spectrometer with a 632.4 nm laser excitation source. Temperature-dependent measurements on pellets were performed using the same device in conjunction with a temperature-controlled Linkam Stage (THMS600).

Temperature-dependent Electrochemical Impedance Spectroscopy

Temperature-dependent dielectric measurements were conducted on pellets inside a liquid N_2-cooled Janis Cryostat over a temperature range of 420K to 100K. Dielectric data was acquired using a Solartron 1296 Dielectric Interface System within a frequency range of 1 MHz to 10 mHz, at an AC applied bias of 100 mV. The sample temperature was maintained with a Lakeshore temperature controller.

Discussion on characterization of Cs_2PtI_6:

The identity of Cs_2PtI_6 was confirmed by comparing the X-ray diffraction pattern with literature data (**Figure S5(a)**). The particle size, visualized using SEM, was found to range between 3-5 µm on average (**Figure S5(b)**). The IR-active stretching and bending modes of the material were measured using Fourier Transform Far-Infrared Spectroscopy (FTIR), revealing two peaks at 180 cm^{-1} and 89.8 cm^{-1}, corresponding to Pt-I asymmetric stretching and I-Pt-I asymmetric bending, respectively (**Figure S5(c)**).

For opto-electronic applications, the absorption onset or bandgap is crucial. The material's absorption onset was observed at 954 nm (**Figure S6(a)**), and the bandgap was determined to be 1.3 eV, calculated from a Tauc plot (**Figure S6(b)**). To investigate phase changes within the stable temperature range, differential scanning calorimetry (DSC) was performed. No phase changes were observed between 180 K and 300 K, as shown in **Figure S7(a)**. The thermogravimetric analysis (TGA) shows that Cs_2PtI_6 remained stable up to approximately 623 K. The material experienced a 60% weight loss, corresponding to the release of two molecules of I_2, leaving behind a residue of Pt and CsI (**Figure S7(b)**).

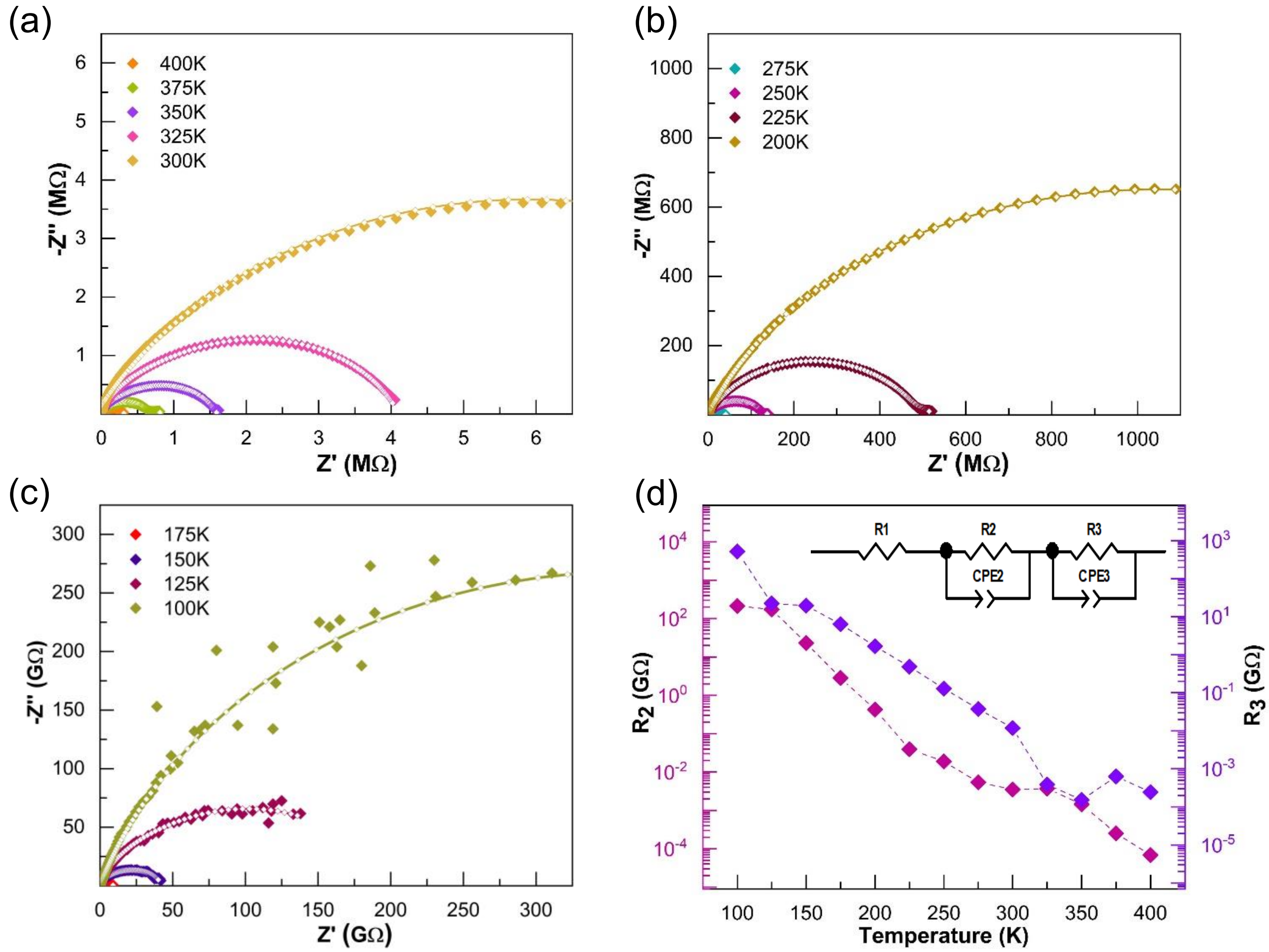

Figure S1. Raw and fit data of the Nyquist plots in the temperature range (a) 400 K ≤ T ≤ 300 K, (b) 275 K ≤ T ≤ 200 K, (c) 175 K ≤ T ≤ 100 K, and (d) temperature-dependence of the charge transport resistances R_2 and R_3 as a function of temperature. The inset shows the equivalent circuit used for fitting the Nyquist plots.

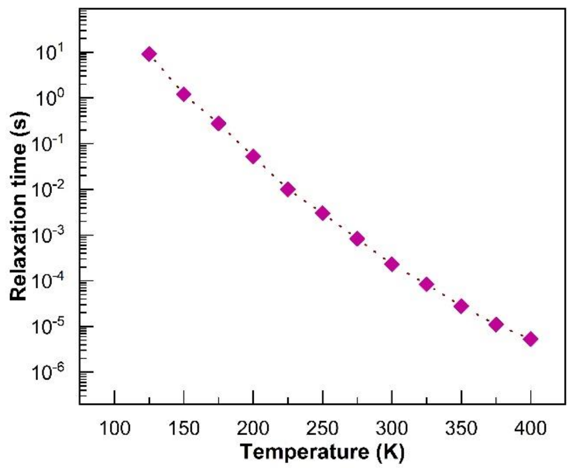

Figure S2. The variation of relaxation time as a function of temperature.

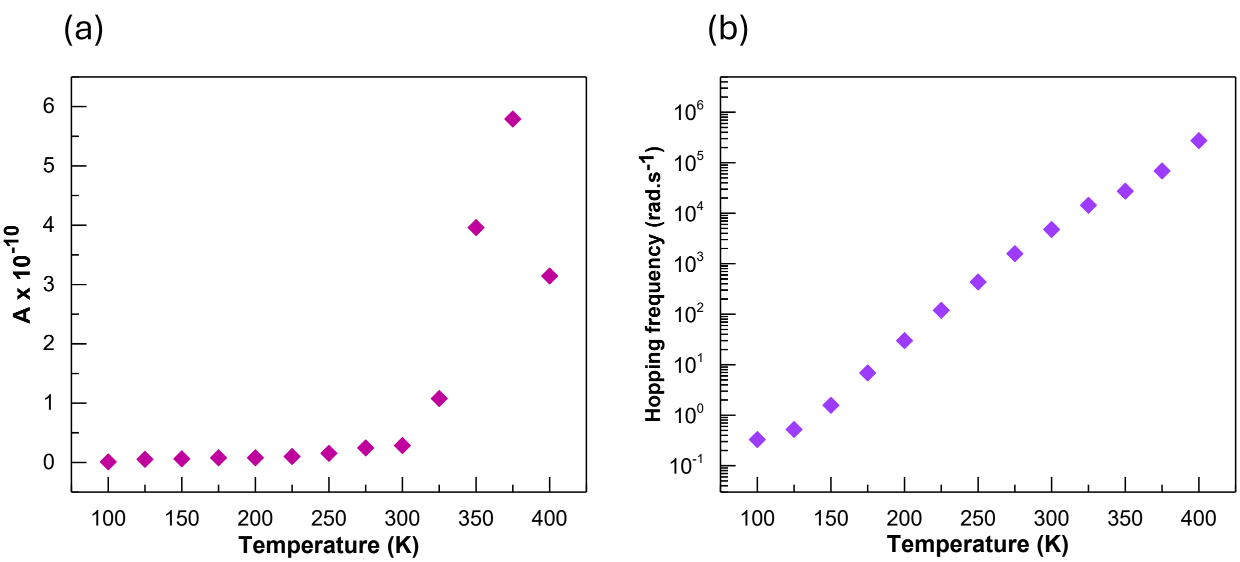

Figure S3. (a) The variation of constant A as a function of temperature and (b) change in hopping frequency with temperature rise.

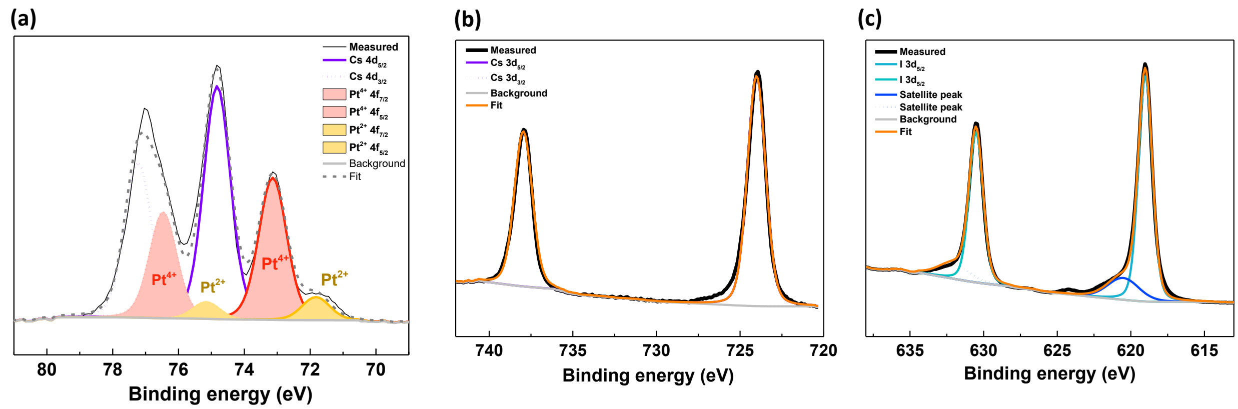

Figure S4. Deconvoluted and fitted X-ray photoemission spectra. (a) Pt *4f* transition (+ Cs *4d* transition, (b) Cs *3d* transition and (c) I *3d* transition.

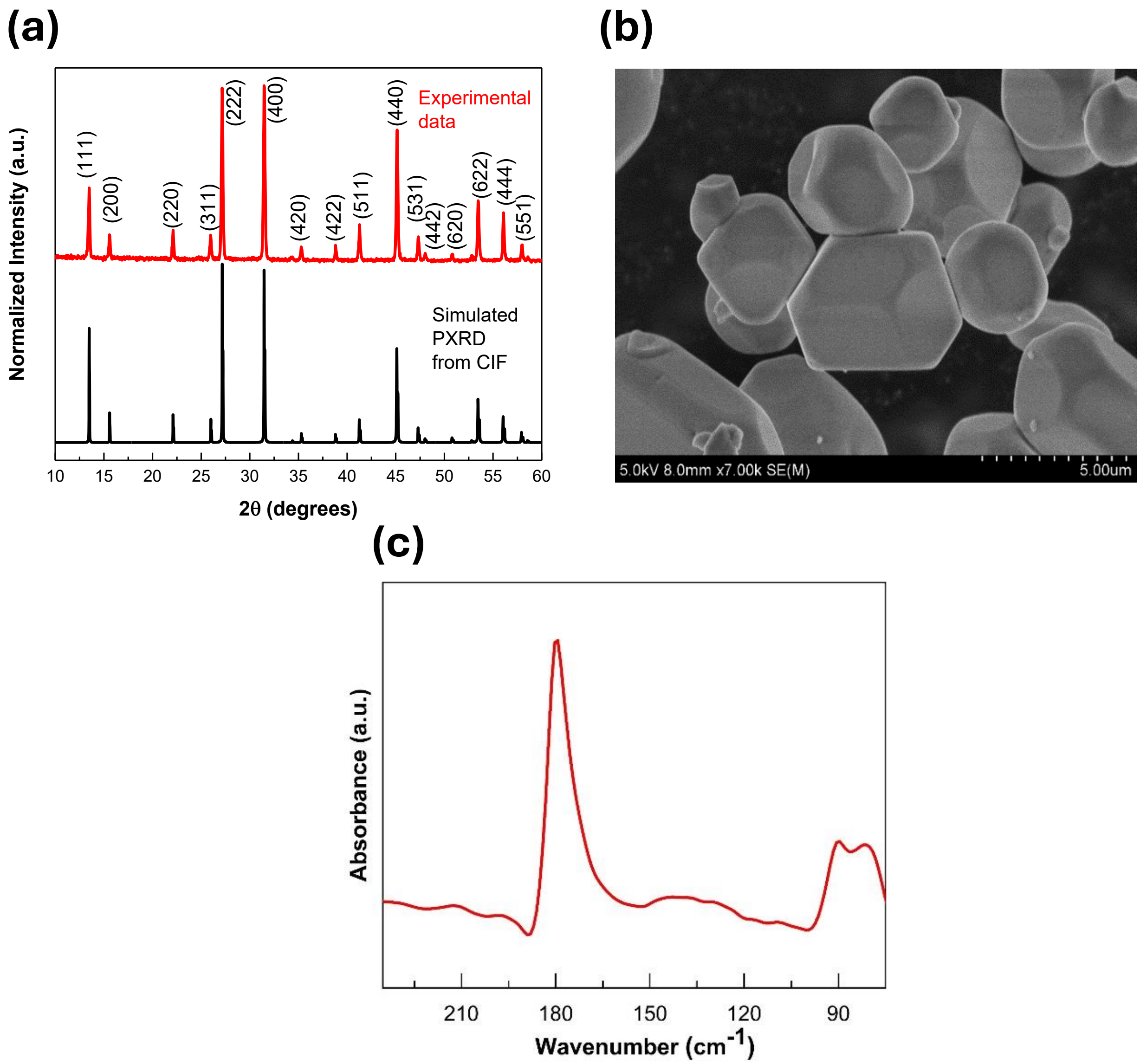

Figure S5. (a) X-ray diffraction (XRD) pattern of synthesized material and its data is compared with simulated XRD from CIF file in reference [1], (b) SEM micrographs, and (c) FTIR data of Cs_2PtI_6.

1 P. Villars and K. Cenzual, Eds., *Springer-Verlag Berlin Heidelberg & Material Phases Data System (MPDS), Switzerland & National Institute for Materials Science (NIMS), Japan*, preprint, https://materials.springer.com/isp/crystallographic/docs/sd_1004269.

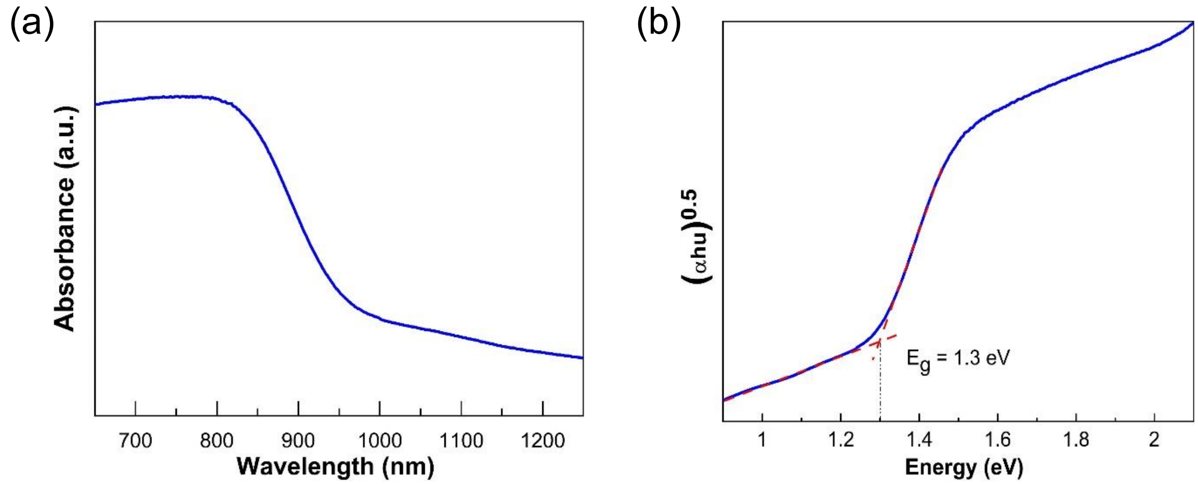

Figure S6. (a) Absorbance spectra of Cs_2PtI_6. (b) Bandgap extracted from Tauc plot.

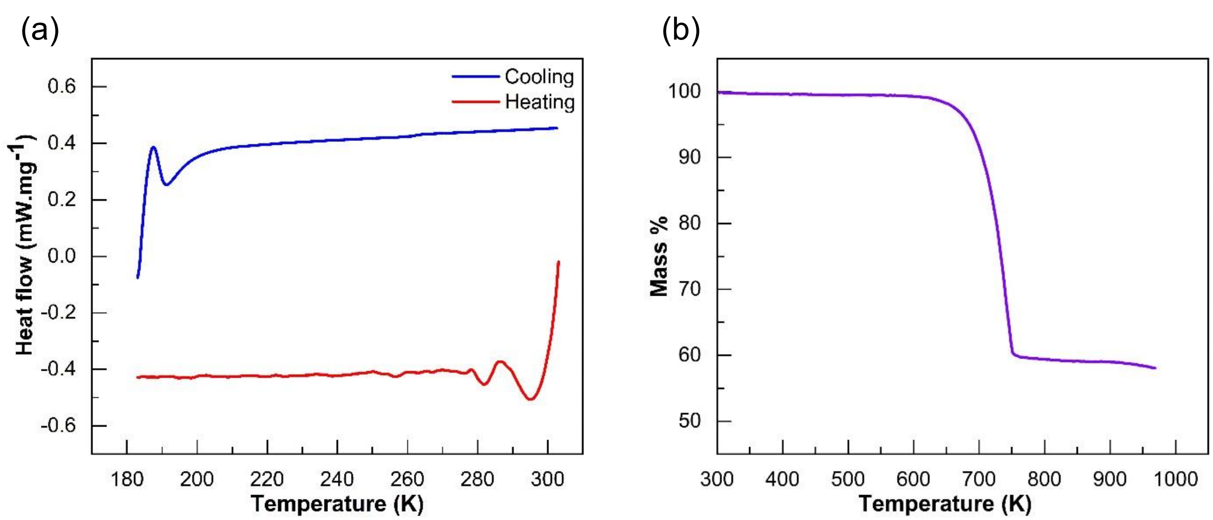

Figure S7. (a) Heat flow in Cs_2PtI_6 obtained during heating and cooling cycles in Differential Scanning Calorimetry measurements and (b) mass loss studied by thermogravimetric analysis of Cs_2PtI_6.